International Journal of Fatigue 180 (2024) 108104

Contents lists available at ScienceDirect

International Journal of Fatigue

journal homepage: www.elsevier.com/locate/ijfatigue

Complete fatigue crack arrest in metallic structures using bonded prestressed iron-based shape memory alloy repairs

Wandong Wang [a,c,*], Wei Zhou [b], Yu'e Ma [a], Masoud Motavalli [c], Elyas Ghafoori [c,d]

[a] School of Aeronautics, Northwestern Polytechnical University, 710072, Xi'an, Shaanxi, PR China
[b] School of Civil Aviation, Northwestern Polytechnical University, 710072, Xi'an, Shaanxi, PR China
[c] Structural Engineering Research Laboratory, Swiss Federal Laboratories for Materials Science and Technology, Empa, 8600, Dübendorf, Switzerland
[d] Institute for Steel Construction, Faculty of Civil Engineering and Geodetic Science, Leibniz University Hannover, 30167, Hannover, Germany

ARTICLE INFO

Keywords:
Fatigue crack arrest
Fe-SMA
Self-prestressing
Adhesive bonding
Fatigue crack retardation

ABSTRACT

Vast aging metallic structures are suffering from fatigue cracking, jeopardizing structural integrity and personnel safety. Therefore it is of great benefit to develop strengthening solutions to achieve complete fatigue crack arrest. A bonded and prestressed fatigue strengthening solution on the basis of an iron-based shape memory alloy (Fe-SMA) shows great potential in this term. An experimental campaign has been carried out in this paper to achieve complete fatigue crack arrest in metallic plates. Several activation methods greatly affecting the prestressing level have been experimentally tested, it has been found that the gas torch activation is the most effective method, extending the fatigue crack growth life by 6.9 times. The experimental campaign has demonstrated that prestressing forces required to achieve complete fatigue crack arrest capability could be realized by increasing the Fe-SMA patch width combined with the most effective activation method. In addition, the results show that the length of the Fe-SMA repair together with the activation length can be reduced without sacrificing the repair efficiency. The findings of this paper are greatly beneficial for industrial sectors suffering from fatigue cracking in metallic structures, small bonded Fe-SMA patches can be easily activated to achieve complete fatigue crack arrest capability.

1. Introduction

Several fatigue strengthening techniques have been developed to combat fatigue deterioration of vast metallic structures, yet a fatigue crack arrest method with great versatility for different industrial sectors is to be developed. Increasing metallic structures in different sectors, such as, infrastructures, offshore structures, aircraft structures etc., are aging and subjected to even more severe service loading, they are highly vulnerable to fatigue cracking which jeopardizes safety of both personnel and structures [1,2]. Fatigue strengthening is a cost-effective yet highly pragmatic solution to ensure structural integrity of vast fatigue cracked structures. Consequently, it has been a vibrant research topic and several techniques have been developed and investigated by researchers [3–8].

Traditionally, fatigue strengthening of metallic structures extends fatigue crack growth life by mechanically attaching metallic patches or adhesively bonding composite patches. The added material provides an additional load path and mitigate the loading at the crack tip. Bonding is preferred over mechanically joining as adhesive bonding provides smoother load distribution and avoids introducing new fatigue sources such as drilled holes. Moreover, adhesive bonding offers a much more effective bridging mechanism and permits the possibility of crack growth monitoring [9]. Nevertheless, the difference in the thermal expansion coefficient of normally used metals and composites leads to tensile residual stresses being formed in the metallic structures, which is detrimental for fatigue strengthening [3,10].

More advanced techniques have also been exploited to achieve fatigue strengthening, such as cold spraying [11,12], wire arc additive manufacturing [13]. In addition to the added material, added load path, beneficial compressive residual stresses can be generated using these methods, which can contribute to retard fatigue crack growth. However, the generated compressive stresses are not sufficient to arrest the crack growth, fatigue crack growth continues under cyclic loading after repairing.

Complete fatigue crack arrest is not unattainable. In order to form sufficient compressive stresses in cracked metallic structures so that

* Corresponding author at: Structural Engineering Research Laboratory, Swiss Federal Laboratories for Materials Science and Technology, Empa, 8600, Dübendorf, Switzerland.
E-mail addresses: w.wang@nwpu.edu.cn (W. Wang), wzhou@mail.nwpu.edu.cn (W. Zhou), ma.yu.e@nwpu.edu.cn (Y. Ma), masoud.motavalli@empa.ch (M. Motavalli), ghafoori@stahl.uni-hannover.de (E. Ghafoori).

https://doi.org/10.1016/j.ijfatigue.2023.108104
Received 19 October 2023; Received in revised form 16 November 2023; Accepted 10 December 2023
Available online 12 December 2023

the crack can be significantly retarded, or even completely arrested, the prestressing technique has been exploited. Prestressing methods, such as mechanically anchoring pre-tensioned carbon fibre reinforced plastics (CFRP) strips [14], bonding CFRP patches with shape memory alloy (SMA) wires embedded [15–18], mechanically anchoring iron-based shape memory alloy (Fe-SMA) strips [19] and bonding Fe-SMA strips [1], have been reported. Very promising results can be found in open literature, Hosseini et al. [20,21] achieved completely crack arrest with prestressed CFRP strips. Zheng and Dawood [16] reported that the fatigue crack extension life can be extended as large as 26 times by prestressing of hybridized SMA and CFRP patches.

The prestressed fatigue strengthening techniques have different working mechanisms. Prestressed CFRP solutions involve pre-tensioning CFRP strips prior to anchoring them to cracked metallic structures, which requires hydraulic jacks and mechanical anchoring [20]. The compressive stresses in parent structures are generated thanks to the mechanism that anchored pre-tensioned CFRP strips tend to spring back elastically. Anchoring pre-tensioned CFRP strips by using adhesive bonding is not a conservatively safe solution as the bondline at the patch tip is subjected to combined severely high prestressing and external loading due to load transfer that can cause premature debonding failure [22,23]. Consequently, a heavy and bulky clamping system is normally required to safely anchor the pre-tensioned CFRP [24]. Modifications to the parent structure in such a solution are not subtle, it is regarded to be more applicable for rigid metallic structures. In addition, buckling of the parent structure due to prestressing also needs to be considered when such a solution is applied [14]. For thin-walled lightweight structures widely used in aerospace and automotive sectors, application of such a prestressed solution is challenging.

Another prestressed solution relies on self-prestressing which takes advantage of the shape memory effect (SME) of SMA. A pre-strained SMA element tries to recover its original shape when heated to its activation temperature, a so-called activation process, prestressing is formed when the recovery deformation is constrained during the activation process [25]. The difficulties associated with the prestressed CFRP solution are circumvented in this method, i.e., no need for the heavy jacks to keep reinforcing materials in tension during the complicated anchoring process. Up to date, both NiTiNb-SMA wires and Fe-SMA strips have been exploited to achieve self-prestressing for fatigue strengthening of metallic structures [1,15,16,19,26,27]. The NiTiNb-SMA wires need to be hybridized with fibre reinforced polymers (FRP) to maximize its repair efficiency, nevertheless, no complete crack arrest using this method has been reported [15,26]. It is noted that the sophisticated hybridization of SMA wires and FRP is time consuming and the NiTi-based SMA material is costly, limiting the vast application of this solution.

An alternative self-prestressing solution is on the basis of the Fe-SMA. Researchers at Swiss Federal Laboratories for Materials science and Technology (EMPA) have recently developed an Fe-17Mn-5Si-10Cr-4Ni-1(V,C) (mass %) SMA particularly for prestressing applications with high recovery stresses [28,29]. A recovery stress as high as 360 MPa can be achieved when a prestrained Fe-SMA member is constrained and activated [29]. Monolithic Fe-SMA can be directly employed for fatigue strengthening as a result of its excellent mechanical properties, fatigue resistance capability and high recovery stresses [1]. Numerous studies have been performed in order to study the effect of prestressed Fe-SMA on fatigue strengthening, as summarized in Ref. [25]. Ghafoori et al. [30] have studies the high-cycle fatigue behavior of the Fe-SMA using constant life diagram method. Lee et al. [31] have studied the effect of restraint condition on the recovery stress of the Fe-SMA. Several activation methods have been employed to activate the Fe-SMA for strengthening purpose, such as gas torch activation method [32], electrical resistance heating (ERH) [19,27], heat gun activation method [1], infrared heating irradiation activation method [33]. The restraint condition and activation temperature are identified to be the key to the prestressing level.

Wang et al. [1] has demonstrated that the bonded prestressed Fe-SMA is feasible and highly effective in terms of retarding fatigue crack growth. The prestressing of the Fe-SMA does not contribute to the stress concentration of the adhesive bondline at the patch tip in this solution owning to the fact that only the middle part of the Fe-SMA patch over the crack in the parent structure is activated, preventing premature debonding failure [1]. In comparison with the mechanically anchored prestressed Fe-SMA solution, not only the repair efficiency is increased by several times thanks to the combined synergistic effect of the prestressing mechanism and bridging mechanism on fatigue crack retardation, but also the bonding technique is preferred over the mechanical joining technique for thin-walled light-weight structures vastly used in aerospace, infrastructure, maritime industries etc. A systematic investigation on the surface preparation methods of the Fe-SMA has been carried out to ensure the integrity of this bonded strengthening solution as well [34]. Nevertheless, it is of great interest to achieve complete crack arrest using this versatile fatigue strengthening solution. To the best of the authors' knowledge, it has not been reported in the open literature that complete crack arrest is achieved using bonded self-prestressed solutions.

The core to the widely accepted crack arrest methods, e.g., stop-hole method, dual-alloy repair method, etc. is to remedy the stress severity at the crack tip by removing the sharp crack tip and adding an additional load path. In terms of adding an additional load path, the bonded prestressed Fe-SMA repair method has the same pros and cons of traditional methods. The essence of the proposed method is to easily generate compressive stresses in the parent structures, which significantly reduces the stress intensity factor at the crack tip without removing the sharp crack tip. The great reduction in the stress intensity factor can then reduce the crack growth rate or even completely arrest the fatigue crack growth.

The objective of the paper is to substantiate the feasibility of achieving complete fatigue crack arrest using the bonded prestressed Fe-SMA strengthening solution. The heating rate and activation temperature are recognized to affect the restraint condition in the bonded Fe-SMA solution, thus affect the prestressing level that can be achieved in the system. This paper therefore studies for the first time the effect of different activation methods on the fatigue crack retardation using bonded prestressed Fe-SMA repairs. The most promising activation method was then exploited to achieve higher prestressing forces for complete fatigue crack arrest. This paper details an extensive fatigue test campaign carried out to study the factors affecting the crack retardation or even crack arrest and discusses the test results and mechanisms of this versatile fatigue strengthening solution. The developed versatile fatigue strengthening solution and experimental results in this paper can be further exploited by industrial sectors to substantially extend service life of metallic structures already containing fatigue cracks.

2. Specimen manufacturing

Several materials and multiple techniques were employed to manufacture specimens used in this research. A detailed explanation of the specimen manufacturing is therefore essential. This section describes the specimen configuration, mechanical properties of involved materials and specimen preparation.

2.1. Specimen configuration

The specimen configuration is illustrated in Fig. 1. A steel plate containing a central notched crack is repaired on both sides by bonding two Fe-SMA strips. The dimensions of the steel plate are provided in Fig. 1. Notch preparation was conducted using electrical-discharge machining (EDM) as per ASTM E 647-00 [35] at Empa. The inset shown in Fig. 1 depicts the detailed dimensions of the notch. The specimen was subjected to fatigue loading before bonding Fe-SMA to generate a

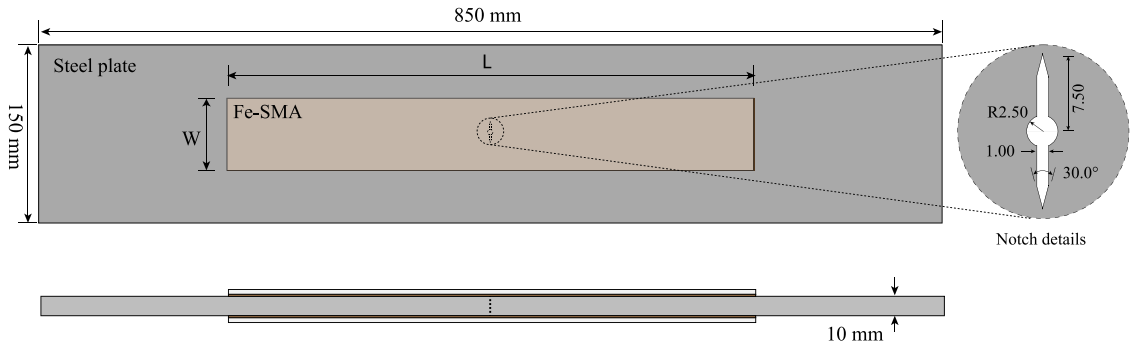

Fig. 1. Schematic configuration of specimen with a central crack.

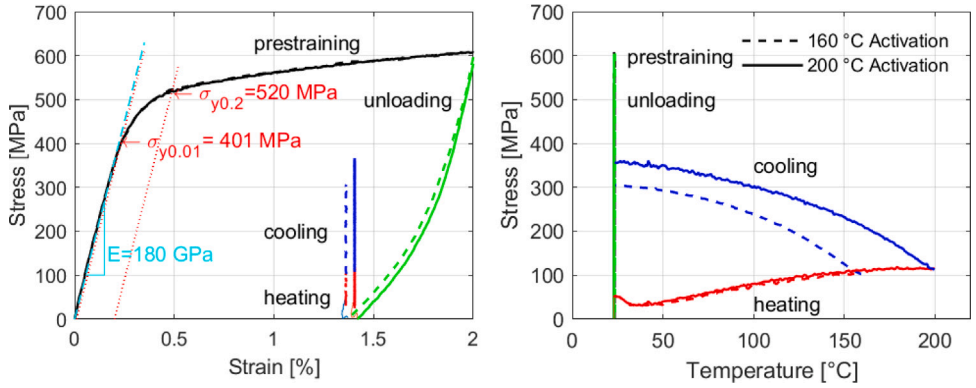

Fig. 2. Thermomechanical behavior of Fe-SMA [1].

precrack length of at least 1 mm [35]. The precracking procedure will be described in detail in Section 3.2.

Two Fe-SMA patches of W in width and L in length were symmetrically bonded on both sides of the steel plate using structural adhesive to study the effect of prestressing on the fatigue life extension. Only the middle part of the Fe-SMA strips of length L_{ac}, the area over the crack, were activated to generate compressive stresses around the crack tip in the steel plate. W, L and L_{AC} are three variables studied in this research work to achieve crack arrest with potentially the smallest Fe-SMA patch size.

2.2. Fe-SMA

The thermomechanical properties of the Fe-SMA lay the cornerstone of achieving fatigue crack arrest with the proposed solution. Consequently, it is essential to understand the behavior of the Fe-SMA when it is subjected to sequential mechanical loading and thermal stimulation for activation. Fig. 2 shows the experimental stress–strain and stress–temperature behavior of the tested Fe-SMA. The Fe-SMA material used in this study is the same as in a previous study [1]. For more details, one is referred to the previous work [1].

For clarity, the thermomechanical behavior of the Fe-SMA is described step-wise. Firstly, the austenite phase, γ, is stable in the pristine Fe-SMA. A 2% prestrain at room temperature is normally applied to the Fe-SMA in the rolling direction. As can be seen from Fig. 2, the Fe-SMA initially exhibits linear behavior and pronounced non-linear behavior starts after about 0.1% strain during the prestraining process. The premature non-linear behavior is attributed to the forward austenite-to-martensite ($\gamma \rightarrow \varepsilon$) transformation [30]. This forward transformation together with plastic deformation leaves a permanent strain after complete unloading the Fe-SMA strip [28].

The strain of the Fe-SMA is kept constant during the activation process, as shown in Fig. 2. To avoid compressive stresses due to thermal expansion in the very beginning of the thermal activation process, a stress level of 50 MPa is applied to the Fe-SMA prior to the activation. During the activation process, thermal expansion dominates on the heating of the Fe-SMA and then SME prevails as temperature increases. Correspondingly, the stress slightly decreases first and increases once the SME dominates. During the cooling process, tensile stresses continue to develop. The non-linearity at the end of the cooling is attributed to the development of new martensite at a high stress level [1]. As shown in Fig. 2, a higher activation temperature leads to a higher recovery stress. It is noted that the contribution of activation duration to the development of recovery stress is negligible.

Table 1
Mechanical properties of the Fe-SMA.

	E [GPa]	σ_y [MPa]	Thickness [mm]
Fe-SMA	180	401	1.5

Based on the tensile stress–strain relationship shown in Fig. 2, the material properties of the Fe-SMA are summarized in Table 1. It is observed from Fig. 2 that the non-linearity of the Fe-SMA starts for strain values smaller than 0.2% owing to the forward phase transformation, so the yield strength, σ_y, is defined for the standard 0.01% yield strength and the Young's modulus is the slope of the curve for a strain value up to 0.1%.

2.3. Steel

The steel plates of grade S355J2+N were utilized for the fatigue test campaign. In total 6 tensile specimens of diameter 6.00 mm were extracted from a steel plate and tensile tests were performed on these specimens according to DIN EN ISO 6892-1:2019 [36] to obtain the mechanical properties. The tensile stress–strain relationships for the 3 tested specimens in the rolling direction and the other 3 tested specimens in the direction perpendicular to the rolling direction are provided in Fig. 3 while the mechanical properties of the steel plates are summarized in Table 2.

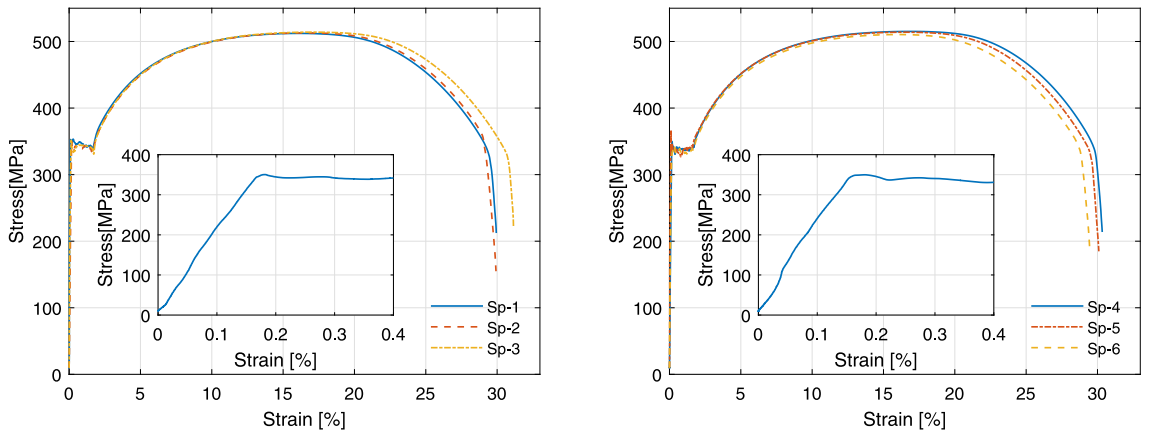

(a) Mechanical behavior in the rolling direction (b) Mechanical behavior in the perpendicular direction

Fig. 3. The stress–strain behavior of steel.

Table 2
Mechanical properties of the steel.

Specimen direction	Elastic modulus [GPa]	Yield stress [MPa]	Ultimate strength [MPa]
Rolling direction	205 ± 2.26	351.55 ± 1.21	513.06 ± 0.94
Perpendicular direction	205 ± 1.58	353.71 ± 11.85	513.19 ± 2.43

2.4. Specimen preparation

The surfaces of the steel plate and the Fe-SMA patches have to be carefully prepared in order to avoid premature debonding failure at the interface between either adherend and the adhesive used. Based on the preliminary study on the debonding failure behavior of bonded Fe-SMA-to-steel joints [37], grit blasting of the steel surfaces and the Fe-SMA surfaces before the application of Sika 1277 adhesive [38] can already achieve cohesive failure. The same surface preparation procedure is therefore adopted in this research project. Prior to grit blasting, the surfaces were thoroughly cleaned by using white clothes soaked with acetone to prevent contamination from spreading to the fresh surfaces during the grit blasting process. A pressure of 8 bar was adopted and 0.15–0.21 mm aluminum oxide was used to grit blast both the steel and Fe-SMA surfaces. After grit blasting, the surfaces were thoroughly cleaned again and the adhesive was applied within 2 h. The Fe-SMA patch and the steel plate were joined together using Sika 1277 adhesive.

The curing of the bonded specimens was carried out in a climate room at Empa laboratory at a controlled temperature of 23 ± 0.5 °C. Weight was placed on the bonded Fe-SMA patches after joining the two adherends to apply a pressure of roughly 0.003 MPa. The specimen was left untouched in the climate room for 14 days in order for the adhesive to be completely cured according to the technical data sheet [38].

The surface preparation and curing of the adhesive were repeated to bond Fe-SMA patches on both sides of the steel plate. The activation of the Fe-SMA was implemented after the adhesive layer was completely cured.

2.5. Activation

Three different activation methods were utilized to activate the Fe-SMA over the crack with the aim of investigating the effect of different activation methods on the fatigue life extension. Fig. 4 shows the three used activation methods, namely, heat gun (HG) activation, hot bonder (HB) activation and gas torch (GT) activation. It is noted that the Fe-SMA on both sides needs to be activated to avoid undesirable secondary bending in this study.

The effect of the three different activation methods on the fatigue life extension was studied by activating the same length of the Fe-SMA patches of different specimens with the same configuration, as shown in Table 3. The activated specimens were then subjected to fatigue loading to reveal their fatigue crack growth behavior and corresponding fatigue lives. The most effective activation method which resulted in the longest fatigue life extension was further employed in combination of larger Fe-SMA patches to achieve fatigue crack arrest. The fatigue test procedure will be detailed in the next section while the procedure of the different activation methods are explained concisely in this subsection.

A heat gun (model: Steinel HG2320E) was used to heat up the target Fe-SMA and the temperature on the surface was monitored using a infrared camera (model: Testo 885) in the HG activation method, as shown in Fig. 4(a). Based on a previous study, it is crucial to paint the Fe-SMA white beforehand in order to have an accurate measurement of the temperature during the activation process [1]. The blowing hot air with a preset temperature of 600 °C, almost the capacity limit of the heat gun, was directed to a specific area until the temperature measured by the infrared camera reached 160 °C and the area next to it was then heated using the same technique. The area over the activation length, L_{AC}, was activated spot-by-spot in this manner manually. For more details, one can refer to the previous study [1].

Fig. 4(b) depicts the hot bonder activation method. A hot bonder (BriskHeat®ACR®3 Hot Bonder, USA) was employed to activate the Fe-SMA, a heating blanket was placed over the area of Fe-SMA to be activated and a vacuum bag was used to hold the heating blanket against the Fe-SMA. Both the vacuum and the heating process were controlled by the hot bonder. A vacuum pressure of 0.86 bar was maintained during the activation process. Several type K thermocouples that were attached to the Fe-SMA surface under the heating blanket were connected to the hot bonder to monitor and control the temperature using a built-in temperature controller. A ramp-up program at the maximum capacity of the hot bonder was employed to heat up the Fe-SMA to a target temperature of 160 °C as fast as possible. However, the heating rate continued to decrease as the temperature increased as a result of heat transfer in the specimen. In the end, the activation was terminated when the measured temperature at the center of the Fe-SMA reached about 155 °C.

The GT activation method, shown in Fig. 4(c), employed a camp gas torch to activate the Fe-SMA to represent an easy on-site activation process without electricity. This activation method is similar to the HG method, flame instead of hot air in this method was directed to a specific area of the Fe-SMA to be activated. White paint could be burned

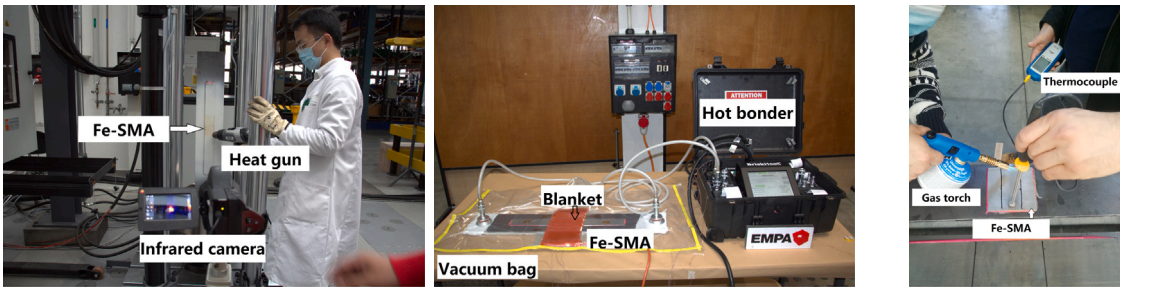

(a) Heat gun (HG) activation (b) Hot bonder (HB) activation (c) Gas torch (GT) activation

Fig. 4. Three different activation methods.

Table 3
Test matrix.

Specimen ID	L [mm]	W [mm]	Activation method	L_{AC} [mm]	a_{pre} [mm]
Ref	–	–	–	–	1.64
N-L-NA[a]	500	50	–	–	1.75
N-L-HG	500	50	HG	150	1.63
N-L-HB	500	50	HB	150	1.57
N-L-GT	500	50	GT	150	1.75
W-L-NA	500	120	–	–	1.54
W-L-GT	500	120	GT	150	1.47
W-M-GT	250	120	GT	100	1.61
W-S-GT	120	120	GT	50	1.63

[a] NA refers to the not activated case.

out and it was not used consequently. The type K thermocouple was employed to measure the temperature of a specific area immediately after heating. The Fe-SMA was considered to be activated once the measured temperature was over 160 °C. Compared to the HG method, the GT activation method is rapid and the temperature that can be reached is much higher. It is crucial to avoid overheating when this method is used to prevent the introduction of damage to the bondline.

3. Fatigue test procedure

An experimental campaign was implemented in order to investigate the effect of bonded prestressed Fe-SMA reinforcements on the fatigue crack growth life extension. A number of specimens with different Fe-SMA configurations were tested under fatigue loading. This section therefore details the test matrix and test procedure.

3.1. Test matrix

Table 3 summarize the test matrix in this work. As discussed in Section 2.1, the length, L, and width, W of the Fe-SMA strips were taken into consideration. The activation method and activation length, L_{AC} were also two key factors to consider. In total 9 specimens were consequently tested. Fatigue test of the same specimen configuration was not repeated owning to extreme time cost.

A coding system is employed to distinguish the specimens in this study. The Ref specimen in Table 3 denotes a bare steel plate containing a central notch that was tested to obtain the reference crack growth behavior. The rest of the specimens in Table 3 is further categorized into two groups. The first group includes specimens reinforced with narrow Fe-SMA strips and the second group includes specimen reinforced with wide Fe-SMA strips.

As shown in Table 3, the specimens in the first group are coded as $N-L-XX$. N and L refer to narrow and long Fe-SMA strips. The dimensions of the Fe-SMA are provided in Table 3. The last two letters in the coding system indicate the activation method. NA refers to the not activated case. This group of specimens with the same Fe-SMA configuration were tested to study the influence of activation method

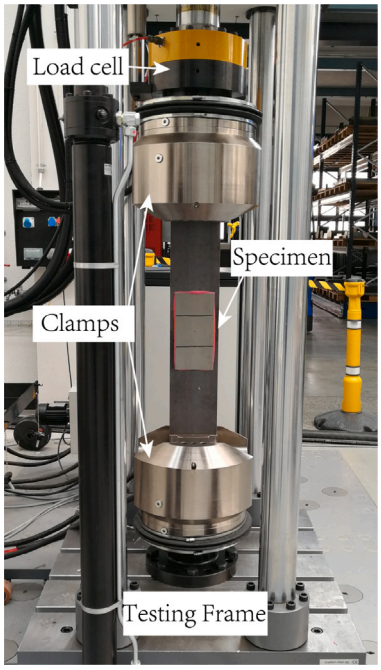

Fig. 5. Fatigue test setup.

on the fatigue crack growth life extension. The most efficient activation method, i.e., the GT method, was chosen to activate the Fe-SMA of the specimens in the second group.

The coding system for the second group is $W-L/M/S-NA/GT$, where W refers to wide Fe-SMA strips, L, M and S refer to long, medium and short Fe-SMA strips. The dimensions are provided in Table 3. It is of great desire to develop repair solutions which can achieve crack arrest for structures with limited space to carry out such repairs. Consequently, the width of the Fe-SMA repairs was kept constant but the Fe-SMA length was reduced together the activation length for the specimens in the second group. The specimens were then tested to realize crack arrest with the smallest Fe-SMA size.

3.2. Pre-cracking

Fatigue pre-cracking was performed to form a sharpened crack tip starting from the EDM notch shown in Fig. 1. Per-cracking serves for two purposes: (1) to form a sharpened crack tip more representative of a realistic crack tip formed in a structure owing to service loading; (2) to minimize the effects of notch manufacturing on the subsequent fatigue crack growth behavior during testing. The fatigue pre-cracking in this research follows the recommendation in ASTM E 647-00 [35]. All the specimens were subjected to the same fatigue loading spectrum

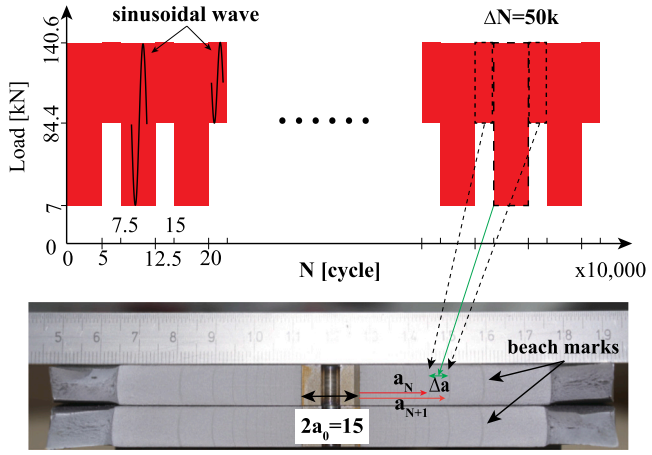

Fig. 6. Illustration of the fatigue spectrum and data processing.

to produce a minimum precrack length of 1.0 mm prior to bonding Fe-SMA patches.

A detailed description of fatigue test is provided in the following section. The difference between pre-cracking tests and fatigue tests lies in the fatigue loading spectrum. The pattern of the fatigue loading spectrum used for pre-cracking is similar to the fatigue loading spectrum used for fatigue tests, as shown in Fig. 6. It is noted that the maximum cyclic force is 140.6 kN while the minimum cyclic force is 28.1 kN for precracking. This loading corresponds to $\Delta\sigma_{pre}$ = 75 MPa with a ratio of R_{pre} = 0.2. This fatigue loading of 50,000 cycles was followed by the beach marking loading of 25,000 cycles with a maximum force of 140.6 kN and a ratio of R = 0.6. The sinusoidal wave shape was used and the loading frequency was 15 Hz. The beach marking technique was adopted to facilitate locating the precrack tip. The beach marking loading dose not advance the crack growth, it leaves a visible mark of the crack front instead. In order to form a minimum precrack of 1 mm, the two alternating blocks of fatigue loading were repeated four times, resulting in a total number of 20 000 cycles of $\Delta\sigma$ = 75 MPa with a ratio of R = 0.2 applied to form a sharpened precrack [1,20]. The resulting precrack lengths are summarized in Table 3. Slight scatter in the precrack lengths can be observed, i.e., the precrack length is 1.62 ± 0.09 mm.

3.3. Fatigue test

The fatigue test set-up is shown in Fig. 5. The fatigue tests were carried out on a computer-controlled servo hydraulic fatigue machine. The specimen was clamped by two sets of wedge grips to a Walter + bai testing frame (type: LFV 500-HH) with a 500 kN load cell (model: GTM DR-F 500 kN). No external fatigue crack detection equipment, such as high resolution cameras, digital image correlation system, was employed to monitor the fatigue crack growth. Beach marking fatigue loading spectrum was utilized to facilitate the fatigue crack growth analysis instead. Constant amplitude fatigue loading spectrum was used. To this end, the machine was tuned to obtain a proper set of PID values for a given specimen configuration before running any fatigue tests.

Fatigue crack growth can eventually fracture the specimen into two halves and the crack surfaces with crack front marks can be exposed. The fatigue loading spectrum together with the crack surfaces shown in Fig. 6 are used to explain how the beach marking technique works. The loading spectrum consists of two alternating blocks of cyclic loading. The maximum cyclic load of 140.6 kN is always the same while the minimum cyclic load values are different. As shown in Fig. 6, the loading with a minimum cyclic load of 7 kN was employed to advance the fatigue crack growth. The ratio of this block of loading is R = 0.05. ΔN_1 = 50,000 was used. The beach marking loading spectrum with R = 0.6 and ΔN_2 = 25,000 was employed to form a visible mark on the crack surface after complete failure of the specimen. The sinusoidal wave shape and a loading frequency of 15 Hz were used as well.

It is noted that a stress ratio of R = 0.2 was used previously for fatigue crack growth [1]. It is argued by the authors that the compressive stresses generated by the bonded and prestressed repair solution mainly changes the stress ratio instead of changing the effective stress intensity factor range of the crack tip [1]. As a result, the fatigue crack growth life enhancement of this bonded and prestressed Fe-SMA repair is not pronounced. When the stress ratio is changed to R = 0.05, as the case in this research, the prestressing effectively shifts the lower part of the applied tensile stress range to negative. Meanwhile, the maximum cyclic stress is also reduced. Consequently, the effective stress range and thus the effective stress intensity factor range experienced by the crack tip after being strengthened is fairly reduced. R = 0.05 was therefore chosen for this fatigue test campaign.

The fatigue test stopped once the steel plate was completely cracked. The specimen was not removed from the fatigue machine immediately as the bonded Fe-SMA patches on both side of the steel plate still joined the two half steel plates. Quasi-static loading was subsequently applied to pull-off the bonded Fe-SMA patches using the fatigue machine. The crack surfaces and the Fe-SMA-to-steel interfaces could then be examined.

Postmortem of the specimen after each fatigue test was performed to attain the crack growth behavior and the bondline failure mechanism. As shown in Fig. 6, a photo of the crack surfaces with a ruler placed above was taken using a 4MP single lens camera. An image processing toolkit ImageJ was used to post-process the images to obtain the crack lengths vs cycles data. The ruler scale was utilized to calibrate the pixel size of the photo and the number of pixels between two given points on the photo could be counted and then the distance can be determined by ImageJ. The distance between the notch tip and a beach mark close to the steel surface was measured. For a given fatigue life, two beach marks could be found on both sides of the initial notch. Four crack lengths were averaged to estimate the crack length. A series of crack lengths corresponding to a fatigue life interval of ΔN_1 = 50,000 could be obtained.

Photos of the damaged surfaces of the bondline between Fe-SMA patches and steel plates were also taken. The morphology of the damaged bondline due to fatigue loading is distinguishable from that due to quasi-static loading [1]. The fractography analysis could reveal the influence of different activation methods on the integrity of bonded Fe-SMA joints subjected to fatigue loading.

4. Results and discussion

The fatigue life extension results and corresponding fatigue crack growth behavior are summarized and analyzed in this section.

The fatigue life extension results are categorized into two groups. The first group exams the influence of the activation methods on the fatigue life extension, their results are summarized in Table 4. The second group exams the feasibility of using small patch sizes to achieve crack arrest, see Table 5. The ratio in the table indicates the fatigue crack growth life ratio between the strengthened specimen and the reference specimen.

As can be seen from Table 4, the activated narrow and long Fe-SMA strips could significantly increase the fatigue crack growth life, but the crack indeed propagated under fatigue loading and cracked the steel plate in the end. Complete fracture of the fatigue strengthened steel plate using narrow and long Fe-SMA configuration was just a matter of time. On the other hand, it shows that the GT activation method resulted in the highest fatigue life extension ratio. The fatigue life extension results of the HG and HB methods are similar.

The crack growth behavior of the tested specimens are analyzed to further deepen the understanding of the prestressing impact on the

Table 4
Fatigue life extension results of narrow Fe-SMA repairs.

Specimen ID	L_{SMA} [mm]	W_{SMA} [mm]	Activation	L_{AC} [mm]	N [10^6 cycle]	Ratio
Ref	–	–	–	–	0.48	–
N-L-NA	500	50	–	–	1.47	3.1
N-L-HG	500	50	HG	150	1.69	3.5
N-L-HB	500	50	HB	150	1.88	3.9
N-L-GT	500	50	GT	150	3.33	6.9

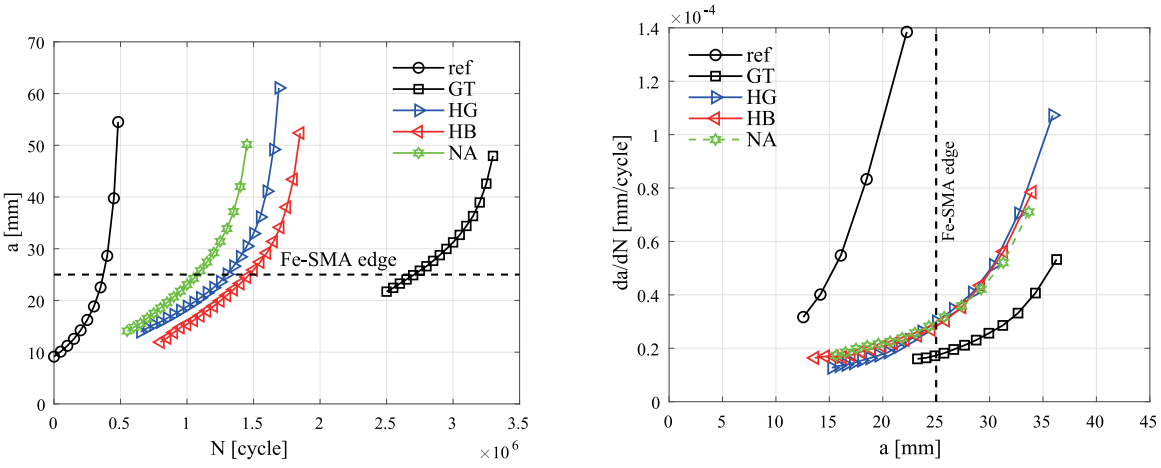

(a) a-N results (b) da/dN-a results

Fig. 7. Three different activation methods.

Table 5
Fatigue life extension results of wide Fe-SMA repairs.

Specimen ID	L_{SMA} [mm]	W_{SMA} [mm]	Activation	L_{AC} [mm]	N [10^6 cycle]	Ratio
Ref	–	–	–	–	0.48	–
W-L-NA	500	120	–	–	2.4	5
W-L-GT	500	120	GT	150	7.1	14.8
W-M-GT	250	120	GT	100	Inf	Inf
W-S-GT	120	120	GT	50	Inf	Inf

fatigue crack retardation. Figs. 7(a) and 7(b) show the a-N and da/dN-a data of the listed specimens in Table 4 respectively. For the fatigue strengthened specimens, the bridging and/or prestressing reduced the loading experienced at the crack tip such that the beaching marking did not leave visible marks for the commencing part of the fatigue crack growth. As the crack propagated, the loading at the crack tip increased and the marks due to beach marking were visible again. The crack growth behavior for crack lengths having visible marks is presented in Fig. 7.

As can be observed from Fig. 7, the crack growth in the bare steel plate is rapid, after initial slow crack growth for several millimeters, the crack growth rate soars up. Bonding non-activated Fe-SMA can reduce the fatigue crack growth rate significantly for the crack growth underneath the Fe-SMA. This reduction in the fatigue crack growth rate is due to the bridging mechanism provided by the bonding technique. Nevertheless, the crack growth rate dramatically increases once the crack tip grows beyond the Fe-SMA edge, which is attributed to the fact that the bridging mechanism is not effective anymore when the crack tip is away from the bridging Fe-SMA. This phenomenon is consistent with the crack growth behavior in fibre metal laminate [39].

In addition to the bridging mechanism, the activation of the Fe-SMA could generate compressive stresses in the cracked steel plate, which further retards the fatigue crack growth. As can be seen from Table 4, the prestressed and bonded Fe-SMA patches consistently lead to longer fatigue crack growth life. Compared to the non-activated case, the HG and HB activation methods lead to 14.97% increase and 27.89% increase in the fatigue crack growth life respectively. As can be observed from Fig. 7, the crack growth rates of these two activated specimens are slightly smaller than that of non-activated specimens when the crack tip is underneath the Fe-SMA patch, once the crack tip is beyond the edge of the Fe-SMA patch, these specimens exhibit highly similar crack growth behavior. It is unfortunate that the crack growth behavior of the commencing part is not available with the beach marking technique. However, it can be observed from Fig. 7(a) that prestressing retard the fatigue crack growth more effectively when the crack length is smaller.

For the GT activated case, the impact of prestressing on the crack growth retardation is much more pronounced, the fatigue crack growth life is twice as much compared to the life of the non-activated case. As can be observed from Fig. 7, not only the growth rate is the lowest when the crack tip is underneath the Fe-SMA patch, but also tremendous retardation effect can be observed when the crack tip grows beyond the patch edge. The highly desirable fatigue crack retardation is attributed to an adequate prestressing level generated by using the GT activation method. Compared to the other two activation methods, the GT activation method could reach a higher temperature instantly without heating up the steel plate and damaging the adhesive layer. Please refer to the postmortem analysis of the bond-line shown in Fig. 10 for more information. Consequently, the promising results motivated

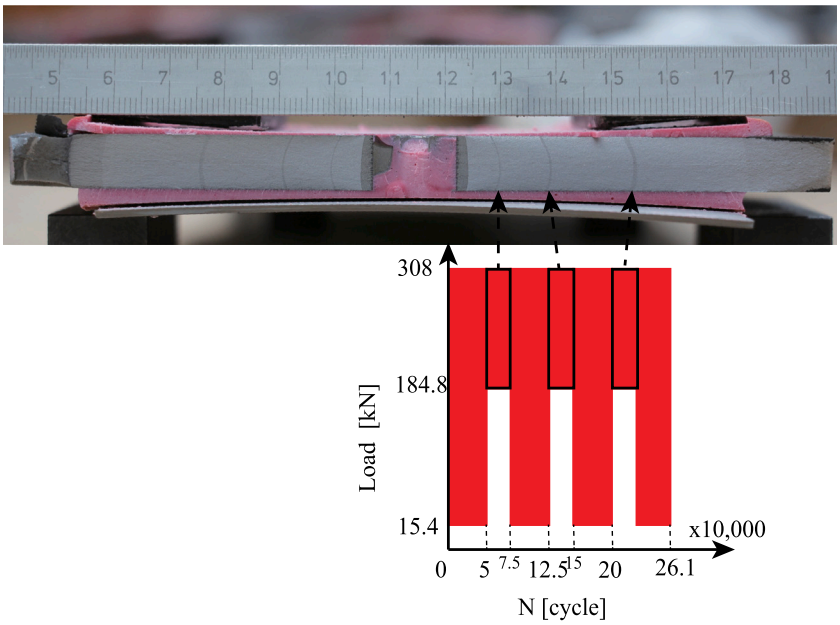

Fig. 8. Postmortem of W-M-GT specimen.

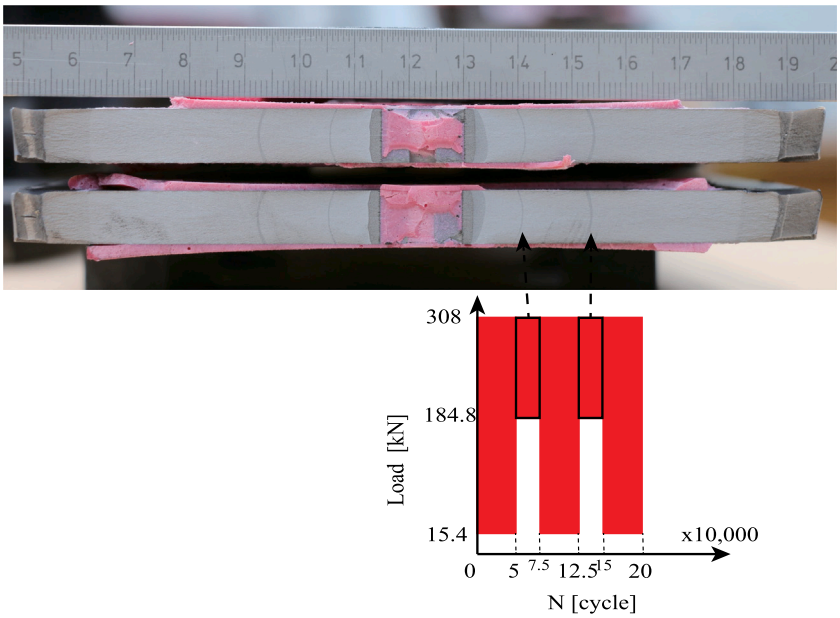

Fig. 9. Postmortem of W-S-GT specimen.

the synergistic combination of the GT activation method and wide Fe-SMA patches to achieve fatigue crack arrest, leading to the fatigue test campaign of the second group of specimens.

The fatigue test results for the second group of specimens are summarized in Table 5. As can be seen, it is feasible to achieve complete fatigue crack arrest using the bonded prestressed Fe-SMA patches. Strengthening the cracked steel plate with wider Fe-SMA patches without the prestressing effect is more efficient in terms of retarding the fatigue crack growth in two ways: (1) more stiffness is added and consequently the loading experienced by the crack tip is less; (2) the bridging mechanism is effective and continues to reduce the stress intensity factor at the crack tip for a much longer crack. The fatigue life results of W-L-NA confirmed the beneficial effect of bonding wide instead of narrow Fe-SMA on retarding the fatigue crack growth, a fatigue crack growth life of 2.4 million cycles was achieved.

The fatigue crack growth lives are tremendously increased for the specimens with activated wide Fe-SMA. The fatigue test was ceased after $1 * 10^7$ cycles for specimens W-M-GT and W-S-GT, no signs of crack increment were found for these two specimens. To reveal the fatigue behavior of these two bonded and prestressed specimens, another fatigue loading spectrum shown in Figs. 8 and 9 were applied. The postmortem images of these two specimens are also provided. As

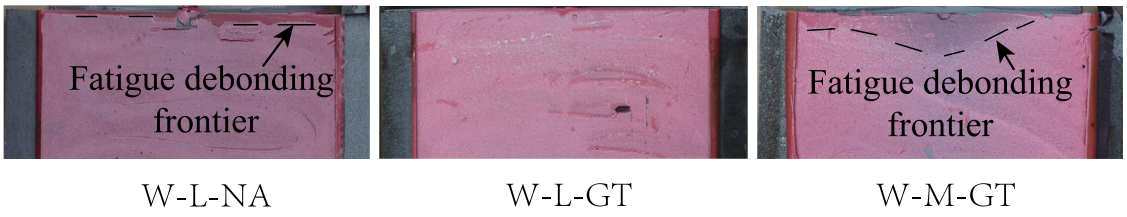

Fig. 10. Postmortem of bondline.

can be seen, the prestressed and bonded Fe-SMA repair solution arrests the fatigue crack growth under the fatigue loading spectrum shown in Fig. 6. After applying the fatigue loading depicted in Fig. 8, the crack starts to grow symmetrically on both sides, three marks due to the beach marking loading can be observed on the crack surface. In total 201,000 cycles of fatigue loading with 308 kN (205.3 MPa) maximum load and R = 0.05 were applied to completely fracture the reinforced steel plate.

Fig. 9 shows the postmortem image of the crack surface of W-S-GT specimen, 1.7 mm crack propagation can be observed on one side of the specimen under the loading spectrum shown in Fig. 6. The crack growth behavior exhibits asymmetry, which is associated with the difference in prestressing generated by the manual activation method on both sides. Nevertheless, the average crack growth is smaller than $1 * 10^{-10}$ m/cycle, implying that the stress intensity factor range is smaller than the threshold and crack arrest is achieved [35]. When the fatigue loading as depicted in Fig. 9 was applied, the crack started to grow. Compared to the W-M-GT specimen, the crack grows faster in W-S-GT and 150,000 cycles of fatigue loading were applied to crack the prestressed reinforced steel plate. The shorter fatigue crack growth life in specimen W-S-GT is mostly attributed to the short patch length in comparison to the W-M-GT specimen. According to the study in Ref. [37], the effective bond length of Fe-SMA bonded joints using Sika 1277 is 115 mm. The crack tip of W-S-GT can be more loaded than that of W-M-GT due to this reason. In addition, the prestressing level in W-S-GT might also be slightly smaller than that in W-M-GT.

Contrary to the crack arrest achieved in W-M-GT and W-S-GT specimens, it is not the case for W-L-GT. Interestingly, the patch length is much longer than the effective bonding length. No crack arrest in this specimen therefore is attributed to a lower prestressing level achieved in W-L-GT than those in W-M-GT and W-S-GT. It is a clear evidence that there are scatters in the prestressing level that can be achieved by using the manual gas torch activation method. Even though crack arrest is not achieved in this specimen, the fatigue crack growth life extension is tremendous, a ratio of 14.8 is achieved as a result of the desirable prestressing effect. It becomes evident that increasing the width of the Fe-SMA patch increases the prestressing forces counteracting the applied loading. The bonded prestressed Fe-SMA strengthening solution arrests fatigue cracks when the prestressing forces developed are high enough.

In addition to the analysis of the crack growth behavior, it is also of great interest to analyze the bondline failure behavior under fatigue loading. Fig. 10 shows typical fractographic images of bondline of representative specimens after the removal of the Fe-SMA patches. It is possible to distinguish the debonding due to fatigue loading from the quasi-static loading, fatigue debonding of the bondline exhibit smoother surface as a result of repetitive friction [1]. As can be seen, debonding due to fatigue loading in W-L-NA and W-L-GT is marginal. It justifies that the gas torch activation does not deteriorate the mechanical properties of the adhesive used. Furthermore, the marginal fatigue debonding in these specimens implies that the bridging mechanism does not weaken during the course of fatigue crack propagation. For specimen W-M-GT, evident fatigue debonding can be observed. However, it is noted that this fatigue debonding is due to the much more severe loading shown in Fig. 8.

5. Conclusions and recommendations

The self-prestressing feature of the Fe-SMA thanks to the SME makes the bonded prestressed Fe-SMA strengthening solution versatile for different metallic structures suffering from fatigue cracking. This paper presents a systematic experimental endeavor to achieve complete fatigue crack arrest in metallic structures using bonded and prestressed Fe-SMA repairs. The experimental results reveal that the developed prestressing forces can be tailored by using different activation methods in combination with Fe-SMA sizes. The prestressing forces required to arrest fatigue cracks in metallic structures can be realized to this end.

For specimens reinforced by bonding Fe-SMA strips of width 50 mm, the gas torch activation method, representing an easy on-site activation approach, was found to be the most effective. This activation method can realize the highest instant temperature in the Fe-SMA than other two activation methods studied, leading to the highest prestressing level and thus tremendous fatigue crack growth life extension. The results show that the fatigue crack growth life was extended by 6.9 times. The developed high prestressing forces continues to greatly retard the fatigue crack growth when the crack tip is beyond the Fe-SMA patch edge. These findings inspired the authors to combine this activation method with Fe-SMA patches of width 120 mm to arrest fatigue crack growth. The experimental results substantiate that the bonded prestressed Fe-SMA solution is able to arrest fatigue cracks in metallic structures. The GT activation method does not deteriorate the mechanical performance of the bondline, but results in high enough prestressing forces so that the fatigue crack is stopped from growing. A small Fe-SMA path configuration as short as 120 mm with an activation length of 50 mm was also tested, complete fatigue crack arrest is achieved as well.

This paper shows the great potential of the bonded prestressed Fe-SMA strengthening solution. Nevertheless, it is noted that more in-depth research is needed to advance this highly efficient strengthening technology. Further study should focus more on the development of analysis tools to reveal the relationship between the bond integrity and the capability of developing prestressing level in the system. The developed analysis tools can then be used to maximize the potential of this repair solution and to analyze possible failure mechanisms of this repair system subjected to very severe loading cases.

CRediT authorship contribution statement

Wandong Wang: Conceptualization, Investigation, Methodology, Writing – original draft. **Wei Zhou:** Formal analysis, Visualization, Writing – review & editing. **Yu'e Ma:** Data curation, Formal analysis, Investigation, Writing – review & editing. **Masoud Motavalli:** Conceptualization, Project administration, Resources, Supervision. **Elyas Ghafoori:** Conceptualization, Funding acquisition, Project administration, Supervision, Writing – review & editing.

Declaration of competing interest

The authors declare the following financial interests/personal relationships which may be considered as potential competing interests: Elyas Ghafoori reports financial support was provided by Innosuisse-Swiss Innovation Agency. If there are other authors, they declare that

they have no known competing financial interests or personal relationships that could have appeared to influence the work reported in this paper.

Data availability

No data was used for the research described in the article.

Acknowledgments

This research was supported by Innosuisse-Swiss Innovation Agency, Switzerland and refer AG with the project number 30060.1 IP-ENG. Dr. Julien Michels has supported the research with in-sightful discussions. The authors would like to thank the technicians of the Empa Structural Engineering Lab for their assistance in performing the experiments. The funding from National Natural Science Foundation of China with the project number 52202509 is also acknowledged for supporting the summarizing and analyzing results of this project.

References

[1] Wang W, Li L, Hosseini A, Ghafoori E. Novel fatigue strengthening solution for metallic structures using adhesively bonded Fe-SMA strips: A proof of concept study. Int J Fatigue 2021;148:106237. http://dx.doi.org/10.1016/j.ijfatigue.2021.106237, URL https://www.sciencedirect.com/science/article/pii/S0142112321000979.

[2] Marazani T, Madyira DM, Akinlabi ET. Repair of cracks in metals: A review. Procedia Manuf 2017;8:673–9. http://dx.doi.org/10.1016/j.promfg.2017.02.086, URL https://www.sciencedirect.com/science/article/pii/S2351978917300926. 14th Global Conference on Sustainable Manufacturing, GCSM 3-5 October 2016, Stellenbosch, South Africa.

[3] Wang W. On the finite width correction factor in prediction models for fatigue crack growth in built-up bonded structures. Eng Fract Mech 2020;107156. http://dx.doi.org/10.1016/j.engfracmech.2020.107156.

[4] Fatigue behaviour of notched steel beams strengthened by a self-prestressing SMA/CFRP composite. Eng Struct 2023;274:115077. http://dx.doi.org/10.1016/j.engstruct.2022.115077.

[5] Barr CM, Duong T, Bufford DC, Milne Z, Molkeri A, Heckman NM, Adams DP, Srivastava A, Hattar K, Demkowicz MJ, Boyce BL. Autonomous healing of fatigue cracks via cold welding. Nature 2023;620(7974):552–6. http://dx.doi.org/10.1038/s41586-023-06223-0.

[6] Wang S, Li L, Su Q, Jiang X, Ghafoori E. Strengthening of steel beams with adhesively bonded memory-steel strips. Thin-Walled Struct 2023;189:110901. http://dx.doi.org/10.1016/j.tws.2023.110901, URL https://www.sciencedirect.com/science/article/pii/S0263823123003798.

[7] Chen Z-Y, Gu X-L, Zhao X-L, Ghafoori E, Yu Q-Q. Fatigue tests on Fe-SMA strengthened steel plates considering thermal effects. J Struct Eng 2023;149(3):04022255. http://dx.doi.org/10.1061/JSENDH.STENG-11694, URL https://ascelibrary.org/doi/abs/10.1061/JSENDH.STENG-11694.

[8] Li L, Wang W, Chatzi E, Ghafoori E. Experimental investigation on debonding behavior of Fe-SMA-to-steel joints. Constr Build Mater 2023;364:129857. http://dx.doi.org/10.1016/j.conbuildmat.2022.129857, URL https://www.sciencedirect.com/science/article/pii/S0950061822035139.

[9] Baker AA. In: Karbhari VM, editor. 2 - Repair of metallic airframe components using fibre-reinforced polymer (FRP) composites. Woodhead Publishing; 2014, p. 11–59. http://dx.doi.org/10.1533/9780857096654.1.11, URL https://www.sciencedirect.com/science/article/pii/B9780857096531500020.

[10] Wang W, Rans C, Benedictus R. Analytical prediction model for fatigue crack growth in fibre metal laminates with MSD scenario. Int J Fatigue 2017;104:263–72. http://dx.doi.org/10.1016/j.ijfatigue.2017.07.024, URL http://www.sciencedirect.com/science/article/pii/S0142112317303225.

[11] Sample CM, Champagne VK, Nardi AT, Lados DA. Factors governing static properties and fatigue, fatigue crack growth, and fracture mechanisms in cold spray alloys and coatings/repairs: A review. Addit Manuf 2020;36:101371. http://dx.doi.org/10.1016/j.addma.2020.101371, URL https://www.sciencedirect.com/science/article/pii/S2214860420307430.

[12] Champagne V, Helfritch D. Critical assessment 11: Structural repairs by cold spray. Mater Sci Technol 2015;31(6):627–34. http://dx.doi.org/10.1179/1743284714Y.0000000723.

[13] Ghafoori E, Dahaghin H, Diao C, Pichler N, Li L, Mohri M, Ding J, Ganguly S, Williams S. Fatigue strengthening of damaged steel members using wire arc additive manufacturing. Eng Struct 2023;284:115911. http://dx.doi.org/10.1016/j.engstruct.2023.115911, URL https://www.sciencedirect.com/science/article/pii/S0141029623003255.

[14] Liu J, Xin H, Zhao X-L. Prediction of fatigue crack propagation in center cracked steel plate strengthened with prestressed CFRP strip. Thin-Walled Struct 2023;183:110416. http://dx.doi.org/10.1016/j.tws.2022.110416, URL https://www.sciencedirect.com/science/article/pii/S0263823122009685.

[15] El-Tahan M, Dawood M, Song G. Development of a self-stressing NiTiNb shape memory alloy (SMA)/fiber reinforced polymer (FRP) patch. Smart Mater Struct 2015;24(6):065035. http://dx.doi.org/10.1088/0964-1726/24/6/065035.

[16] Zheng B, Dawood M. Fatigue strengthening of metallic structures with a thermally activated shape memory alloy fiber-reinforced polymer patch. J Compos Constr 2017;21(4):04016113. http://dx.doi.org/10.1061/(ASCE)CC.1943-5614.0000776.

[17] Deng J, Fei Z, Wu Z, Li J, Huang W. Integrating SMA and CFRP for fatigue strengthening of edge-cracked steel plates. J Constr Steel Res 2023;206:107931. http://dx.doi.org/10.1016/j.jcsr.2023.107931, URL https://www.sciencedirect.com/science/article/pii/S0143974X2300158X.

[18] Li L, Chen T, Gu X, Ghafoori E. Heat activated SMA-CFRP composites for fatigue strengthening of cracked steel plates. J Compos Constr 2020;24(6):04020060. http://dx.doi.org/10.1061/(ASCE)CC.1943-5614.0001072.

[19] Izadi MR, Ghafoori E, Motavalli M, Maalek S. Iron-based shape memory alloy for the fatigue strengthening of cracked steel plates: Effects of re-activations and loading frequencies. Eng Struct 2018;176:953–67. http://dx.doi.org/10.1016/j.engstruct.2018.09.021, URL http://www.sciencedirect.com/science/article/pii/S0141029618305042https://ac.els-cdn.com/S0141029618305042/1-s2.0-S0141029618305042-main.pdf?_tid=0685f32a-fdd6-47c6-88ab-c48ac69f48ad&acdnat=1542646137_2d32ec9fac4179eb111a9ce9af9aeb7f.

[20] Hosseini A, Ghafoori E, Motavalli M, Nussbaumer A, Zhao X-L. Mode I fatigue crack arrest in tensile steel members using prestressed CFRP plates. Compos Struct 2017;178:119–34. http://dx.doi.org/10.1016/j.compstruct.2017.06.056, URL http://www.sciencedirect.com/science/article/pii/S0263822317309248.

[21] Hosseini A, Nussbaumer A, Motavalli M, Zhao X-L, Ghafoori E. Mixed mode I/II fatigue crack arrest in steel members using prestressed CFRP reinforcement. Int J Fatigue 2019;127:345–61. http://dx.doi.org/10.1016/j.ijfatigue.2019.06.020.

[22] Hosseini A, Ghafoori E, Wellauer M, Sadeghi Marzaleh A, Motavalli M. Short-term bond behavior and debonding capacity of prestressed cfrp composites to steel substrate. Eng Struct 2018;176:935–47. http://dx.doi.org/10.1016/j.engstruct.2018.09.025.

[23] Martinelli E, Hosseini A, Ghafoori E, Motavalli M. Behavior of prestressed CFRP plates bonded to steel substrate: Numerical modeling and experimental validation. Compos Struct 2019;207:974–84. http://dx.doi.org/10.1016/j.compstruct.2018.09.023.

[24] Hosseini A, Ghafoori E, Motavalli M, Nussbaumer A, Zhao X-L, Al-Mahaidi R. Flat prestressed unbonded retrofit system for strengthening of existing metallic I-Girders. Composites B 2018;155:156–72. http://dx.doi.org/10.1016/j.compositesb.2018.08.026, URL http://www.sciencedirect.com/science/article/pii/S1359836818312848.

[25] Hosseini A, Michels J, Izadi M, Ghafoori E. A comparative study between Fe-SMA and CFRP reinforcements for prestressed strengthening of metallic structures. Constr Build Mater 2019;226:976–92. http://dx.doi.org/10.1016/j.conbuildmat.2019.07.169, URL https://www.sciencedirect.com/science/article/pii/S0950061819318434.

[26] Zheng B, Dawood M. Debonding of carbon fiber-reinforced polymer patches from cracked steel elements under fatigue loading. 2016;20(6):04016038 http://dx.doi.org/10.1061/(ASCE)CC.1943-5614.0000694.

[27] Izadi M, Hosseini A, Michels J, Motavalli M, Ghafoori E. Thermally activated iron-based shape memory alloy for strengthening metallic girders. Thin-Walled Struct 2019;141:389–401. http://dx.doi.org/10.1016/j.tws.2019.04.036.

[28] Lee WJ, Weber B, Feltrin G, Czaderski C, Motavalli M, Leinenbach C. Phase transformation behavior under uniaxial deformation of an Fe–Mn–Si–Cr–Ni–VC shape memory alloy. Mater Sci Eng A 2013;581:1–7. http://dx.doi.org/10.1016/j.msea.2013.06.002, URL https://www.sciencedirect.com/science/article/pii/S0921509313006266.

[29] Lee WJ, Weber B, Feltrin G, Czaderski C, Motavalli M, Leinenbach C. Stress recovery behaviour of an Fe–Mn–Si–Cr–Ni–VC shape memory alloy used for prestressing. Smart Mater Struct 2013;22(12):125037, URL http://stacks.iop.org/0964-1726/22/i=12/a=125037.

[30] Ghafoori E, Hosseini E, Leinenbach C, Michels J, Motavalli M. Fatigue behavior of a Fe-Mn-Si shape memory alloy used for prestressed strengthening. Mater Des 2017;133:349–62. http://dx.doi.org/10.1016/j.matdes.2017.07.055, URL https://www.sciencedirect.com/science/article/pii/S0264127517307311.

[31] Lee WJ, Weber B, Leinenbach C. Recovery stress formation in a restrained Fe–Mn–Si-based shape memory alloy used for prestressing or mechanical joining. Constr Build Mater 2015;95:600–10. http://dx.doi.org/10.1016/j.conbuildmat.2015.07.098, URL http://www.sciencedirect.com/science/article/pii/S0950061815301197https://ac.els-cdn.com/S0950061815301197/1-s2.0-S0950061815301197-main.pdf?_tid=fe03d69e-f552-49d6-b552-a5cd1991e69f&acdnat=1542291285_d8422441c44a57b6e10fdc3bf1678840.

[32] Hothifa R, Raafat E-H. Self-prestressing using iron-based shape memory alloy for flexural strengthening of reinforced concrete beams. ACI Struct J 2017;114(2). http://dx.doi.org/10.14359/51689455.

[33] Fritsch E, Izadi M, Ghafoori E. Development of nail-anchor strengthening system with iron-based shape memory alloy (Fe-SMA) strips. Constr Build Mater 2019;229:117042. http://dx.doi.org/10.1016/j.conbuildmat.2019.117042.

[34] Pichler N, Wang W, Poulis JA, Ghafoori E. Surface preparations and durability of iron-based shape memory alloy adhesively-bonded joints. Int J Adhes Adhes 2023;125:103439. http://dx.doi.org/10.1016/j.ijadhadh.2023.103439, URL https://www.sciencedirect.com/science/article/pii/S0143749623001197.

[35] ASTM. Standard test method for measurement of fatigue crack growth rates. ASTM E647-00, West Conshohocken, PA: American Society for Testing and Materials; 2000.

[36] ISO E6892-1. Metallic materials — tensile testing — Part 1: Method of test at room temperature, Vol. 2019. Standard, International Organization for Standardization; 2019.

[37] Wang W, Hosseini A, Ghafoori E. Experimental study on Fe-SMA-to-steel adhesively bonded interfaces using DIC. Eng Fract Mech 2021;244:107553. http://dx.doi.org/10.1016/j.engfracmech.2021.107553, URL http://www.sciencedirect.com/science/article/pii/S0013794421000308.

[38] SikaPower-1277 Product data sheet. Product data sheet, Zurich, Switzerland: Sika Services AG; 2018.

[39] Wang W, Rans C, Alderliesten RC, Benedictus R. Predicting the influence of discretely notched layers on fatigue crack growth in fibre metal laminates. Eng Fract Mech 2015;145:1–14. http://dx.doi.org/10.1016/j.engfracmech.2015.06.062, http://www.sciencedirect.com/science/article/pii/S0013794415003288http://ac.els-cdn.com/S0013794415003288/1-s2.0-S0013794415003288-main.pdf?_tid=223fa1e6-62bd-11e5-811f-00000aacb361&acdnat=1443100196_e58453b1056e3d208d2116871b0138b3.